ORIGINAL ARTICLE
http://dx.doi.org/10.5653/cerm.2012.39.2.58
pISSN 2233-8233 · eISSN 2233-8241
Clin Exp Reprod Med 2012;39(2):58-67

CERM

Function of the pentose phosphate pathway and its key enzyme, transketolase, in the regulation of the meiotic cell cycle in oocytes

Yunna Kim[1], Eun-Young Kim[1], You-Mi Seo[1], Tae Ki Yoon[2], Woo-Sik Lee[2], Kyung-Ah Lee[1,2]

[1]Department of Biomedical Science, College of Life Science, CHA University; [2]CHA Research Institute, Fertility Center, CHA General Hospital, Seoul, Korea

Objective: Previously, we identified that transketolase (*Tkt*), an important enzyme in the pentose phosphate pathway, is highly expressed at 2 hours of spontaneous maturation in oocytes. Therefore, this study was performed to determine the function of *Tkt* in meiotic cell cycle regulation, especially at the point of germinal vesicle breakdown (GVBD).
Methods: We evaluated the loss-of-function of *Tkt* by microinjecting *Tkt* double-stranded RNAs (dsRNAs) into germinal vesicle -stage oocytes, and the oocytes were cultured *in vitro* to evaluate phenotypic changes during oocyte maturation. In addition to maturation rates, meiotic spindle and chromosome rearrangements, and changes in expression of other enzymes in the pentose phosphate pathway were determined after *Tkt* RNA interference (RNAi).
Results: Despite the complete and specific knockdown of *Tkt* expression, GVBD occurred and meiosis was arrested at the metaphase I (MI) stage. The arrested oocytes exhibited spindle loss, chromosomal aggregation, and declined maturation promoting factor and mitogen-activated protein kinase activities. The modified expression of two enzymes in the pentose phosphate pathway, *Prps1* and *Rbks*, after *Tkt* RNAi and decreased maturation rates were amended when ribose-5-phosphate was supplemented in the culture medium, suggesting that the Tkt and pentose phosphate pathway are important for the maturation process.
Conclusion: We concluded that Tkt and its associated pentose phosphate pathway play an important role in the MI-MII transition of the oocytes' meiotic cell cycle, but not in the process of GVBD.

Keywords: Oocyte; Meiosis; RNA interference; Transketolase; Pentose phosphate pathway

Introduction

Mammalian oocytes are arrested at prophase I in the ovarian follicles, but undergo spontaneous maturation without requiring any stimulation factors upon removal from the follicle [1]. Progression of oocyte maturation through metaphase I (MI), which leads to chromatin condensation and spindle assembly, and MII occur without an intervening S phase [2].

We previously investigated global gene expression during oocyte maturation at 2 hours intervals and found that 417 genes were differentially expressed around the time of germinal vesicle breakdown (GVBD). Among these genes, five are involved in carbohydrate metabolism, and three, glucose phosphate isomerase 1 (*Gpi1*), glucose-6-phosphate dehydrogenase 2 (*G6pd2*), and transketolase (*Tkt*), are related to the pentose phosphate pathway. It has been reported that the pentose phosphate pathway may regulate oocyte maturation and early development of the embryo [3-5]. However, those results were obtained from the cumulus-oocyte complex (COC) and embryos, in a study that did not observe the molecular and cellular process-

Received: Jun 4, 2012 · Revised: Jun 11, 2012 · Accepted: Jun 16, 2012
Corresponding author: **Kyung-Ah Lee**
CHA Research Institute, Fertility Center, CHA General Hospital, 6-9 Nonhyeon-ro 105-gil, Gangnam-gu, Seoul 135-081, Korea
Tel: +82-2-557-3937 Fax: +82-2-563-2028 E-mail: leeka@ovary.co.kr

***This work was supported by a grant of the Korea Healthcare Technology R&D Project, Ministry for Health, Welfare & Family Affairs, Republic of Korea (A084923) and by the Priority Research Centers Program through the National Research Foundation of Korea (NRF) funded by the Ministry of Education, Science and Technology (2009-0093821).**

es in the oocyte itself. Therefore, it is necessary to examine the role of the pentose phosphate pathway in the oocyte in relation to oocyte maturation.

The pentose phosphate pathway meets the need of all organisms for a source of nicotinamide adenine dinucleotide phosphate (NADPH) to use in reductive biosynthesis, such as fatty acid, cholesterol, neurotransmitter, and nucleotide biosynthesis, and synthesizes five-carbon sugars (Figure 1). *Tkt,* with the transaldolase (*Taldo1*), is an enzyme in the nonoxidative branch of the pentose phosphate pathway that connects it with glycolysis, providing sugar phosphates to the main carbohydrate metabolic pathways [6]. Hexokinase phosphorylates glucose to form glucose-6-phosphate (G6P), an intermediate for either glycolysis or the pentose phosphate pathway. The pentose phosphate pathway converts G6P into ribulose-5-phosphate (Ru5P). Isomerization and epimerization reactions transform Ru5P either to xylulose-5-phosphate or to R5P, and R5P is converted into phosphoribosyl-pyrophosphate (PRPP), which enters into the de novo purine synthetic pathway [7]. It has been suggested that the purine nucleotides participate in the adenylate cyclase-catalyzed production of cyclic adenosine monophosphate (cAMP), which is a well-known regulator of oocyte maturation [8,9].

Energy substrates are key elements in the mechanism that controls oocyte maturation [4]. Therefore, we hypothesized that the loss of *Tkt* would have a detrimental effect on the spontaneous maturation of denuded oocytes, and we evaluated the consequence of the loss of *Tkt* on oocyte maturation, especially on the resumption of meiosis, by the microinjection of *Tkt* double-stranded RNAs (dsRNAs) into germinal vesicle (GV) oocytes.

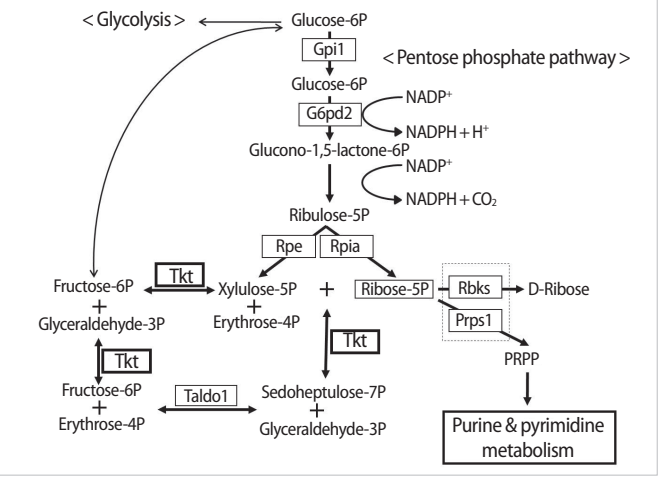

Figure 1. Diagram of the pentose phosphate pathway showing substrates and enzymes involved in it. *Tkt*, transketolase; *Gpi1*, glucose phosphate isomerase 1; *G6pd2*, glucose-6-phosphate dehydrogenase 2; *Rpe*, ribulose-5-phosphate-3-epimerase; *Rpia*, ribose 5-phosphate isomerase A; *Taldo1*, transaldoase 1; *Rbks*, ribokinase; *Prps1*, phosphoribosyl pyrophosphate synthetase 1.

Methods

1. Animals and collection of mouse oocytes

All ICR mice were acquired from Koatech (Pyeongtaek, Korea). This research was approved by the Institutional Animal Care and Use Committee of CHA University. For the collection of GV-stage oocytes from preovulatory follicles, three-week-old female ICR mice were injected with 5 IU of equine chorionic gonadotropin (eCG) and then sacrificed 46 hours later. After removal of the ovaries, the COCs were recovered in dishes of M2 medium (Sigma, St. Louis, MO, USA) containing 0.2 mM 3-isobutyl-1-methylxanthine (IBMX, Sigma), which was used to inhibit GVBD. Cumulus cells (CCs) were removed by repeated passage of the oocytes through a fine-bore pipette.

For the collection of the MII-stage oocytes, female mice were injected with 5 IU eCG and, 46 hours later, with 5 IU hCG. Ovulated MII oocytes were collected from the oviduct 16 hours after the hCG injection. The CCs surrounding the MII oocytes were removed by treating COCs with hyaluronidase (300 U/mL, Sigma).

2. Isolation of mRNA

Messenger RNA was isolated from oocytes using the Dynabeads mRNA DIRECT Kit (Invitrogen Dynal AS, Oslo, Norway). To evaluate mRNA recovery, 0.1 ng green fluorescent protein (GFP) synthetic RNA was added to each oocyte prior to mRNA extraction. Briefly, GV-MII oocytes were resuspended in 300 μL lysis/binding buffer (100 mM Tris-HCl [pH 7.5], 500 mM LiCl, 10 mM ethylenediaminetetraacetic acid [EDTA], 1% SDS, 5 mM dithiothreitol [DTT]) for 3 minutes at room temperature. After vortexing, 20 μL of prewashed Dynabeads Oligo $(dT)_{25}$ were mixed with lysate and annealed by rotating for 3 minutes at room temperature. The beads were separated with a Dynal MPC-S magnetic particle concentrator, and poly $(A)^+$ RNA was eluted by incubation in 14 μL of Tris-HCl (10 mM Tris-HCl, pH 7.5) at 70°C for 2 minutes.

3. Preparation of double-stranded RNA

Tkt cDNA, amplified using the *Tkt*-A primer (Table 1), was cloned into the pGEM-T Easy Vector (Promega, Madison, WI, USA) and linearized with SpeI. The orientation of the insert was confirmed by polymerase chain reaction (PCR) amplification using the T7 primer with each *Tkt*-A primer. Sequences of RNA were synthesized using T7 polymerase and the MEGAscript Kit (Ambion, Austin, TX, USA). Single-stranded sense and antisense transcripts were mixed, incubated at 75°C for 5 minutes, and then cooled to room temperature. Synthesis of dsRNA was confirmed using 1% agarose gel electrophoresis.

4. Reverse transcriptase-PCR

Complementary DNA (cDNA) was synthesized from mRNA using

Table 1. Primer sequences and RT-PCR conditions

Gene	Primer sequence[a]	Annealing temperature (℃)
Tkt-A[a]	F-TCCACCGTCTTTTACCCAAG	60
	R-CAAGGCCTCATGCAGAGTTA	
Tkt-B[b]	F-TCGGAGCTCTTCAAAAAGGA	60
	R-TCTCTGTTGCAACTCCATCG	
Plat	F-CATGGGCAAGAGTTACACAG	60
	R-CAGAGAAGAATGGAGACGAT	
Mos	F-TGGCTGTTCCTACTCATTTC	60
	R-CTTTATACACCGAGCCAAAC	
Rpia	F-TGCAGCGAATAGCTGAAAGA	60
	R-ACAGCCATTCGAAGTTCCAC	
Taldo1	F-TGACGCTCATCTCTCCCTTT	60
	R-GCCAGCTTGCTGTTATCCTT	
Rpe	F-GGGGAATGGGATGAAGGTT	60
	R-GCACTGCCAGACACAATCAT	
G6pd2	F-CTGAATGAACGCAAAGCTGA	60
	R-CAATCTTGTGCAGCAGTGGT	
Gpi1	F-GTGGTCAGCCATTGGACTTT	60
	R- CTTTCCGTTGGACTCCATGT	
Rbks	F-AGTGGCTGGAGCAAATCTGT	60
	R-GCGTGGCCTGTTAAAATCTC	
Prps1	F-TTGATATCCCGGTGGACAAT	60
	R-AGGGCCAGAAAAGATTCCAT	
H1foo	F-GCGAAACCGAAAGAGGTCAGAA	60
	R-TGGAGGAGGTCTTGGGAAGTAA	
GFP	F-ATGGTGAGCAAGGGCGAG	60
	R-CTTGTACAGCTCGTCCAT	

RT-PCR, reverse transcriptase-polymerase chain reaction; F, forward; R, reverse.
[a]Primers were used for RT-PCR and preparation of dsRNA; [b]Primers were used to confirm the knockdown of *Tkt* mRNA after RNAi.

the SuperScript Preamplification System Protocol (Gibco-BRL, Grand Island, NY, USA). Then, mRNA was incubated with 0.5 μg dT primer at 70°C for 10 minutes. The reverse transcription reaction was carried out in M-MLV RT 5X Buffer (250 mM Tris-HCl [pH 8.3], 373 mM KCl, 15 mM $MgCl_2$, 50 mM DTT), 0.5 mM of each deoxyribonucleotide triphosphate (dNTP), and 200 U of M-MLV Reverse Transcriptase (Promega), in a 20 μL final volume. The reaction mixture was incubated at 42°C for 90 minutes, and then at 94°C for 2 minutes. Single oocyte cDNA was used as a template for the PCR analysis. The PCR conditions and primer sequences for the genes encoding *Plat, Mos, Rpia, Taldo1, Rpe, G6pd2, Gpi1, Rbks, Prps1, H1foo* (the internal control), *GFP* (as the external control), and *Tkt*-B are listed in Table 1. The PCR products were then separated by 1.5% agarose gel electrophoresis.

5. Quantitative real-time RT-PCR

Quantitative real-time RT-PCR analysis was performed using the iCycler (Bio-Rad Laboratories Inc., Hercules, CA, USA). The iQ SYBR Green Supermix PCR reagents (Bio-Rad Laboratories Inc.) were used for monitoring amplification and the results were evaluated with iCycler iQ real-time detection system software. The reaction mixture contained cDNA, 20 pmol forward and reverse primers, and SYBR Green Supermix 2 (100 mM KCl, 40 mM Tris-HCl [pH 8.4], 0.4 mM of each dNTP, 50 U/mL iTaq DNA polymerase, 6 mM $MgCl_2$, SYBR Green I, 20 nM fluorescein, and stabilizers). The template was amplified with 40 cycles of denaturation at 95°C for 40 seconds, annealing at 60°C for 40 seconds, and extension at 72°C for 40 seconds. Upon completion of PCR, fluorescence was monitored continuously while slowly heating the samples from 60°C to 95°C at 0.5°C intervals. The melting curves were used to identify any nonspecific amplification performed by determining the cycle threshold (C_T) based on the fluorescence detected within the geometric region of the semi-log amplification plot. Expression of each mRNA species was normalized to that of GFP synthetic RNA. Relative quantitation of the target gene expression was evaluated using the comparative C_T method [10] and the experiments were repeated at least three times using different sets of oocytes.

6. Microinjection and *in vitro* culture

To determine the function of Tkt in oocyte maturation, *Tkt* dsRNA was microinjected into the cytoplasm of GV oocytes. Oocytes were microinjected with 10 pL of *Tkt* dsRNA (2.3 μg/μL) in M2 medium containing 0.2 mM IBMX using a constant-flow system (Femtojet; Eppendorf, Hamburg, Germany). As a control to evaluate any injection damage, oocytes were injected with elution buffer. To determine the rate of maturation *in vitro*, the microinjected GV oocytes were cultured in M16 medium for 16 hours or in M16 medium containing 0.2 mM IBMX for 8 hours, followed by a further 16 hours in M16 medium in 5% CO_2 at 37°C.

7. Non-invasive observation of the spindle structure

The spindle structures of the living oocytes were observed using the LC Pol-Scope optics and controller system combined with a computerized image analysis system (Oosight Meta Imaging System, CRI Inc., Woburn, MA, USA).

8. Orcein and immunofluorescence staining

The oocytes were fixed in aceto-methanol (acetic acid : methanol = 1 : 3) solution for at least 3 to 4 hours at 4°C. The fixed oocytes were mounted on slides, stained with aceto-orcein solution (1% Orcein, 45% acetic acid), and examined under microscopy.

Immunofluorescence staining for α-tubulin and DNA was performed as described previously [10]. Denuded oocytes were placed in Dulbecco's phosphate-buffered saline (PBS) containing 0.1% PBS- polyvinyl alcohol (PVA), 4% paraformaldehyde, and 0.2% Triton X-100, and then fixed for 40 minutes at room temperature. The fixed oocytes were washed 3 times in PBS-PVA for 10 minutes each time and stored overnight in 1% bovine serum albumin (BSA)-supplemented

http://dx.doi.org/10.5653/cerm.2012.39.2.58

PBS-PVA (BSA-PBS-PVA). The oocytes were blocked with 3% BSA-PBS-PVA for 1 hour and incubated with the mouse monoclonal anti-α-tubulin antibody (1:100 dilution, sc-8035; Santa Cruz Biotechnology, Santa Cruz, CA, USA) at 4°C overnight. After washing, the oocytes were incubated with fluorescein isothiocyanate-conjugated anti-mouse IgG (1:40; Sigma) for 1 hour at room temperature, and the DNA was counterstained with propidium iodide (Sigma).

9. Dual kinase activity assay

The activities of two important kinases, maturation promoting factor (MPF) and mitogen-activated protein kinase (MAPK), involved in oocyte maturation were assayed simultaneously in each sample. The dual kinase assay was conducted as described previously [10]. The oocytes were washed in 0.1% PBS-PVA, and each group of oocytes was placed in an Eppendorf tube containing 1 μL of 0.1% PBS-PVA and 4 μL of ice-cold extraction buffer. The oocytes were centrifuged at 13,000 g for 3 minutes, added to 5 μL of kinase buffer (containing 0.3 μCi/mL γ-[^{32}P]-ATP, Amersham Pharmacia Biotech, Buckinghamshire, UK) and 5 μL of substrate solution, and this mixture was incubated for 20 minutes at 37°C. The substrate solution for the MPF and MAPK dual kinase assay contained 4.5 μL of histone H1 (5 mg/mL, from calf thymus) and 0.5 μL of myelin basic protein (MBP; 5 mg/mL, from bovine brain). The reaction was terminated by the addition of 5 μL of 4X SDS sample buffer and boiling for 5 minutes. The samples were loaded onto a 15% gel for separation of the labeled MBP and histone H1, followed by drying of the gels and autoradiography.

10. Statistical analysis

The data were analyzed with one-way analysis of variance. The results are presented as the mean ± SE and a *p*-value of less than 0.05 was considered statistically significant.

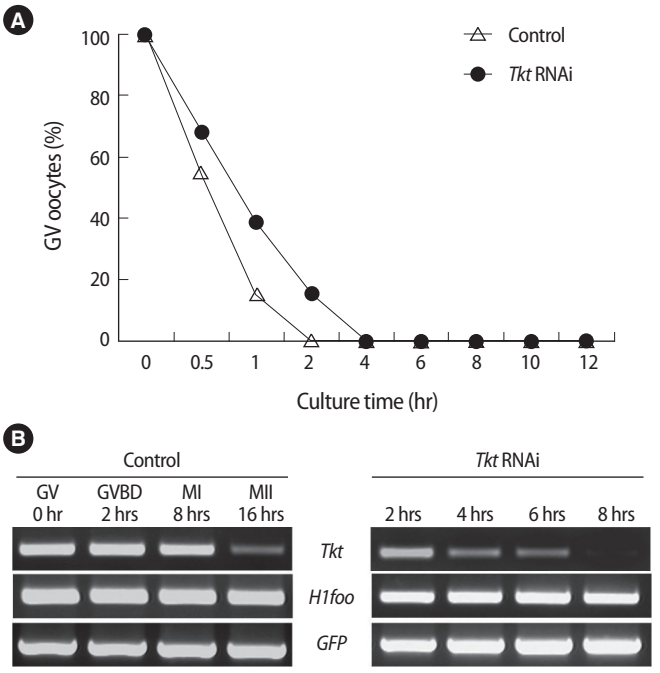

Figure 3. Effect of *Tkt* RNAi on oocyte maturation. (A) Time-dependent maturation of oocytes. (B) *Tkt* mRNA expression during normal *in vitro* maturation (left panel), and degradation of *Tkt* mRNA by *Tkt* RNAi treatment (right panel). *H1foo* and *GFP* mRNA represent an internal and external control, respectively. *Tkt*, transketolase; *H1foo*, H1 histone family, member O, oocyte-specific; *GFP,* green fluorescent protein; GV, germinal vesicle; GVBD, germinal vesicle breakdown; MI, metaphase I; MII, metaphase II.

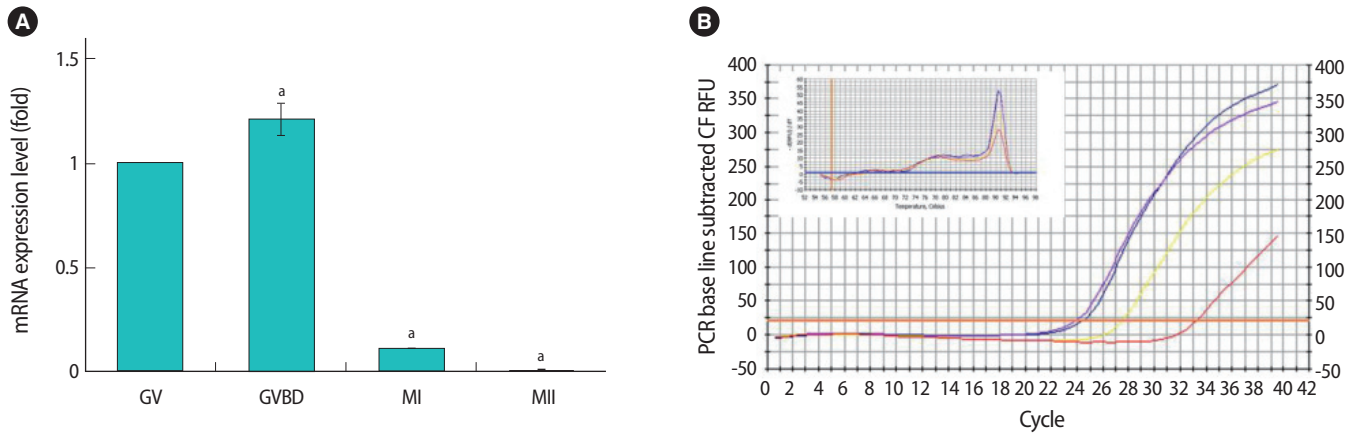

Figure 2. Quantitative real-time reverse transcriptase-polymerase chain reaction of *Tkt* mRNA during *in vitro* maturation. (A) Data are expressed as mean ± SE relative to the value obtained for GV oocytes. The experiments were repeated at least 3 times. (A) indicates a statistical difference compared to the GV ($^{a}p < 0.05$). (B) Amplification profile of *Tkt* showing its C_T value for each stage. The graph in the inner box shows the neat and clean melting curves for amplified *Tkt* confirming the pure product of *Tkt*. *Tkt*, transketolase; GV, germinal vesicle; GVBD, germinal vesicle breakdown; MI, metaphase I; PCR, polymerase chain reaction; CF RFU, curve fit relative fluorescence unit.

Results

1. Oocyte maturation after *Tkt* RNAi

Using real-time RT-PCR, we confirmed that the expression of *Tkt* mRNA was the highest at GVBD (Figure 2). We evaluated changes in oocyte maturation at 0.5 hour intervals during the first 2 hours of dsRNA microinjection, and at 2 hours intervals for the ensuing 16 hours. Unexpectedly, GVBD occurred in the absence of *Tkt* expression. However, GVBD was slightly retarded compared to that of the

Table 2. *In vitro* maturation of mouse oocytes following *Tkt* dsRNA microinjection into GV oocytes

	Number of oocytes (%)				
	Total	Germinal vesicle	Metaphase I	Metaphase II	Abnormal
Control	110	0 (0.0)	6 (5. 5)	104 (94.5)	0 (0.00)
Buffer	157	1 (0.6)	19 (12.1)	137 (87.3)	0 (0.00)
Tkt dsRNA	168	3 (1.8)	126 (75.0)[a]	6 (3.6)[a]	33 (19.6)[a]

Tkt, transketolase; dsRNAs, double-stranded RNAs; GV, germinal vesicle.
[a]$p < 0.05$ compared to the control or buffer-injected group.

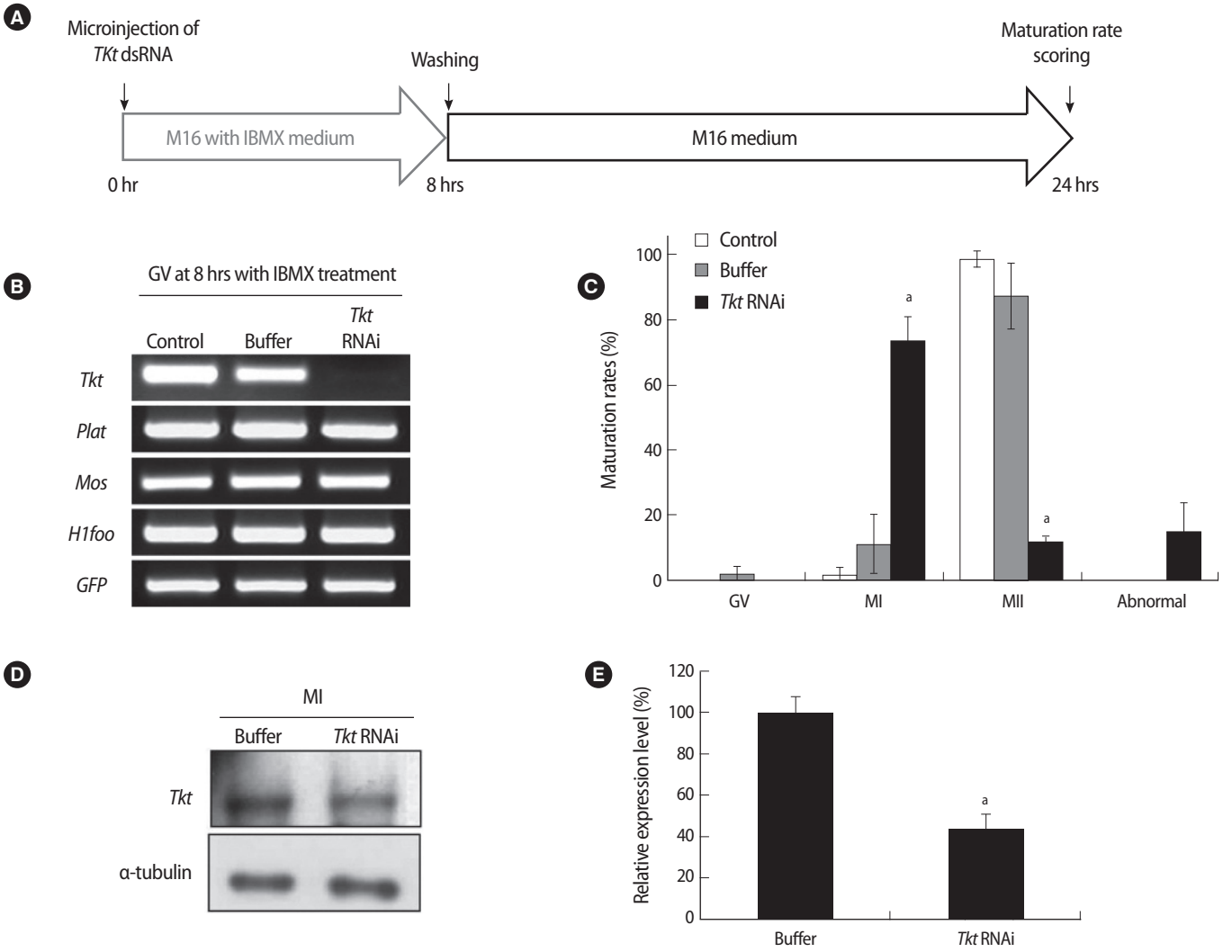

Figure 4. Effects of complete knockdown of *Tkt* mRNA on oocyte maturation. (A) Schematic diagram of the experimental strategy. After microinjection of *Tkt* dsRNA, oocytes were cultured in M16 medium containing 3-Isobutyl-1-methylxanthine (IBMX) for 8 hours and subsequently for 16 hours in IBMX-free M16 culture medium. (B) Confirmation of *Tkt* mRNA knockdown at the GV stage by RT-PCR. (C) Maturation rate of oocytes. The alphabet a represents a significant difference compared to the appropriate value of the control groups ($p < 0.05$). The experiments were repeated at least 3 times. (D) Western blot analysis in MI oocytes after RNAi and (E) its densitometric analysis ([a]$p < 0.05$). Alpha-tubulin was used as a loading control. IBMX, 3-Isobutyl-1-methylxanthine; *Tkt*, transketolase; plat, plasminogen activator, tissue; Mos, c-mos proto-oncogene; *H1foo*, H1 histone family, member O, oocyte-specific; *GFP*, green fluorescent protein; GV, germinal vesicle; RT-PCR, reverse transcriptase-polymerase chain reaction; MI, metaphase I; MII, metaphase II.

http://dx.doi.org/10.5653/cerm.2012.39.2.58

control oocytes, but finally all oocytes resumed meiosis at around 4 hours of incubation (Figure 3A). The maturation rate to MII (3.57%) significantly decreased after *Tkt* RNAi compared to that of the control oocytes (94.55%). Seventy-five percent of oocytes subjected to RNAi treatment were arrested at the MI stage, and 19.64% of oocytes had an abnormal shape (Table 2). The typical expression pattern of *Tkt* mRNA during *in vitro* maturation exhibited a remarkable reduction in the MII stage (Figure 3B). In comparison, the *Tkt* mRNA levels began to decline gradually at 4 hours and completely disappeared by 8 hours in culture after RNAi treatment (Figure 3C). Thus, we decided to incubate the oocytes after RNAi in the IBMX-containing medium for 8 hours to ensure complete degradation of *Tkt* at the GV stage, and then to start *in vitro* maturation without *Tkt* mRNA expression.

After 8 hours of incubation in IBMX-containing medium, an additional 16 hours of culture in IBMX-free M16 medium was followed to allow *in vitro* maturation, as described in Figure 4A. Complete knockdown of *Tkt* mRNA in the oocytes at the GV stage was confirmed after 8 hours of incubation (Figure 4B). By incubation in IBMX-free medium for 16 hours, we confirmed the resumption of meiosis of those oocytes despite the complete knock down of *Tkt* mRNA. Again, approximately 80% of the oocytes were arrested at the MI stage (Figure 4C). Western blot analysis of Tkt protein in MI-arrested oocytes showed a marked decrease (around 60%) of Tkt protein expression by *Tkt* RNAi (Figure 4D, E).

2. Changes in the spindle and chromosomes after *Tkt* RNAi

We analyzed the state of the meiotic spindles non-invasively in living oocytes using a Pol-Scope (Figure 5A). The control oocytes had bright barrel-shaped spindles in a normal position (Figure 5Aa'). The spindles in all of the *Tkt* RNAi oocytes were undetectable with the Pol-Scope (Figure 5Ab', c'). The chromosomes also exhibited an abnormal aggregated form by *Tkt* knockdown (Figure 5Ae, f). We confirmed these abnormal features of the spindles and chromosomes again by immunofluorescence staining (Figure 5Ag-i). By immunofluorescence staining, it was apparent that the spindle structure was severely affected by *Tkt* RNAi.

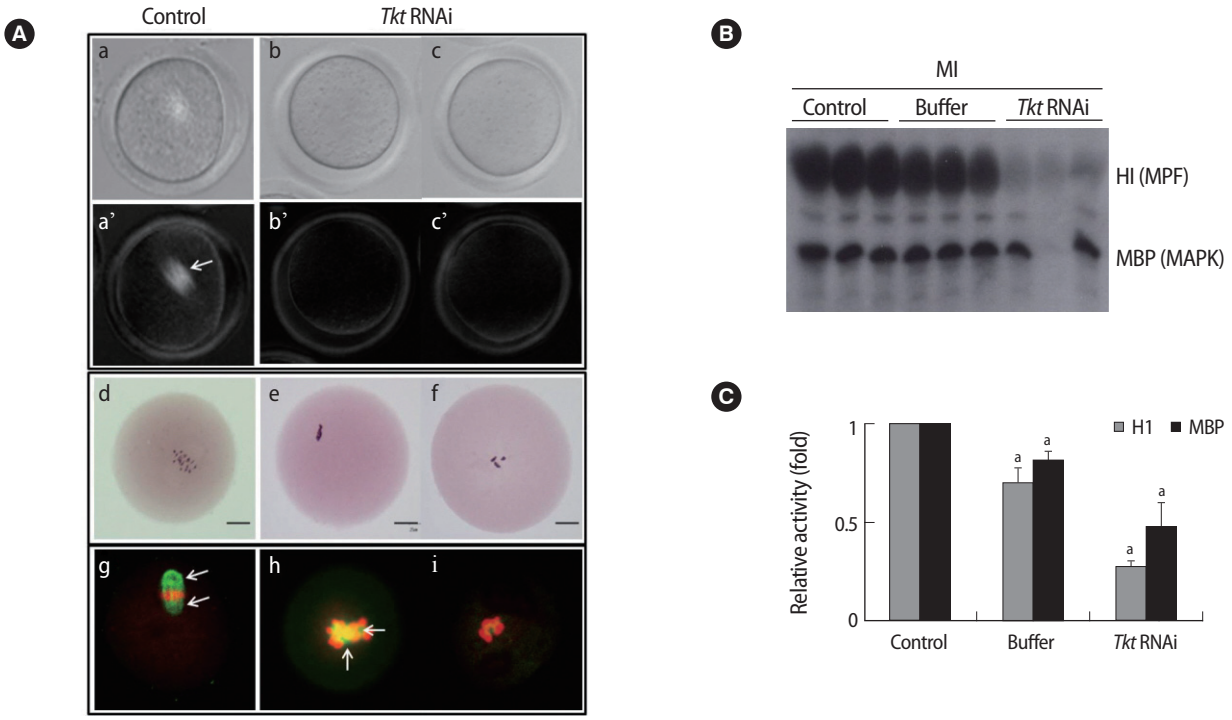

Figure 5. Changes in spindle, chromosome, and kinase activity in oocytes after *Tkt* RNAi. (A) Spindle structure of control MI (a) and arrested MI oocytes (b, c) was observed non-invasively following microinjection of *Tkt* dsRNA using a Pol-Scope. Upper column: bright fields; lower column: dark fields. Chromosome status was evaluated by Orcein staining (d-f). Bars indicate 25 μm. The abnormalities in the spindles and chromosomes in the *Tkt* RNAi oocytes (h, i) were confirmed by immunofluorescence staining. Green, tubulin; red, DNA. Arrows indicate spindles. (B) The amount of substrate phosphorylation following *Tkt* RNAi treatment. Phosphorylation of the substrates H1 and MBP reflects the kinase activities of MPF and MAPK, respectively. Each lane contains one oocyte of the indicated group. (C) The amount of phosphorylated H1 and MBP, namely the relative activity of each kinase, was calculated by quantifying phosphorylation of the substrates. The experiments were repeated at least three times, and the data are presented as the mean ± SE ($^a p < 0.05$). *Tkt*, transketolase; MPF, maturation promoting factor; MAPK, mitogen-activated protein kinase; H1, histone H1; MBP, myelin basic protein; MI, metaphase I.

To investigate the interrelationship between *Tkt* RNAi and the two well-known regulators of oocyte maturation, MPF and MAPK, we measured the activities of these two kinases. The activities of these two kinases were measured by examining histone H1 and MBP phosphorylation as a substrate for MPF and MAPK, respectively. Each lane of Figure 5B represents the activities of the two kinases in a single MI oocyte. Both kinases' activities decreased significantly in the *Tkt* RNAi group (Figure 5C). This strongly suggests that *Tkt* RNAi resulted in disturbed kinase systems.

3. Changes in expression of other enzymes in the pentose phosphate pathway after *RNAi*

Tkt catalyzes the conversion of sedoheptulose-7P to R5P, which is the substrate for enzymes Prps1 and Rbks (Figure 1). When *Tkt* mRNA was completely knocked down, the expression of other enzymes' transcripts (*Gpi1, G6pd2, Rpe, Rpia*, and *Taldo*) in the pathway was not affected, but *Prps1* and *Rbks* transcripts were dramatically decreased (Figure 6). Therefore, we hypothesized that this decrease of *Prps1* and *Rbks* mRNA expression may have been caused by *Tkt* RNAi and by its consequence of a decreased amount of substrate R5P. We then confirmed this hypothesis by culturing oocytes in the medium supplemented with 1 mM R5P, as described in the schematic diagram in Figure 7A. After *Tkt* RNAi, 16.7% of oocytes reached MII in M16 medium, whereas 38.5% of oocytes developed to the MII stage when cultured in the medium containing 1 mM R5P (Figure 7B). We also found increased *Rbks* and *Prps1* mRNA expression in the R5P-treated oocytes (Figure 7C, *Tkt* RNAi+R5P lane).

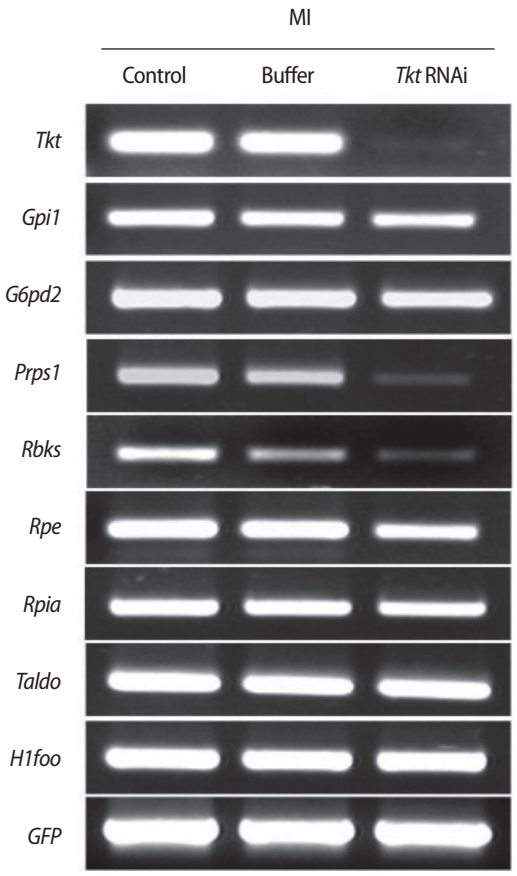

Figure 6. Changes in the expression of enzymes involved in the pentose phosphate pathway by *Tkt* RNAi. *Tkt*, transketolase; *Gpi1*, glucose phosphate isomerase 1; *G6pd2*, glucose-6-phosphate dehydrogenase 2; *Prps1*, phosphoribosyl pyrophosphate synthetase 1; *Rbks*, ribokinase; *Rpe*, ribulose-5-phosphate-3-epimerase; *Rpia*, ribose 5-phosphate isomerase A; *Taldo1*, transaldoase 1; *H1foo*, H1 histone family, member O, oocyte-specific; *GFP*, green fluorescent protein; MI, metaphase I.

Discussion

Tkt, an enzyme in the non-oxidative branch of the pentose phosphate pathway, is an important enzyme that has been reported to be related to many diseases, such as the loss of eye transparency, Alzheimer's disease, cancer, and diabetes [11-14]. By serving as a reversible linkage between the pentose phosphate pathway and glycolysis, Tkt permits the cell to adapt to a variety of metabolic needs under changing circumstances [14]. Tkt is necessary for embryonic development, since it is essential for energy production and nucleic acid synthesis [15]. We hypothesized that Tkt and its related metabolic pathway, the pentose phosphate pathway, may play important roles in oocyte maturation, especially in the commencement of GVBD, since we had confirmed that *Tkt* mRNA expression is highest at GVBD by real-time PCR. However, contrary to this assumption, complete knockdown of *Tkt* mRNA at the GV stage did not affect the initiation of GVBD in mouse oocytes. Even though we obtained complete mRNA knocked down by RNAi, the oocytes still had a remnant of around 40% of Tkt protein, even though it is supposed to be an endogenous protein that existed from the starting point, that is, prior to the RNAi. Thus, to clarify the possible role of endogenous protein on the initiation of GVBD, we examined the effect of complete inhibition of the pentose phosphate pathway on the GVBD by using a pentose phosphate pathway inhibitor. When we completely blocked the pentose phosphate pathway by using 100 nM diphenyleneiodonium, an inhibitor of NADPH oxidase used as a pentose phosphate pathway inhibitor [16], added to the oocyte culture medium, it still did not affect the initiation of GVBD (data not shown). Therefore, we concluded that Tkt and/or the pentose phosphate pathway are not associated with the nuclear membrane breakdown of the oocytes, the initiation step of the meiotic resumption.

Although it is dispensable to GVBD, meiotic cell cycle progression did require Tkt and the normal pentose phosphate pathway because the *Tkt* knocked down oocytes arrested at the MI stage with abnor-

http://dx.doi.org/10.5653/cerm.2012.39.2.58

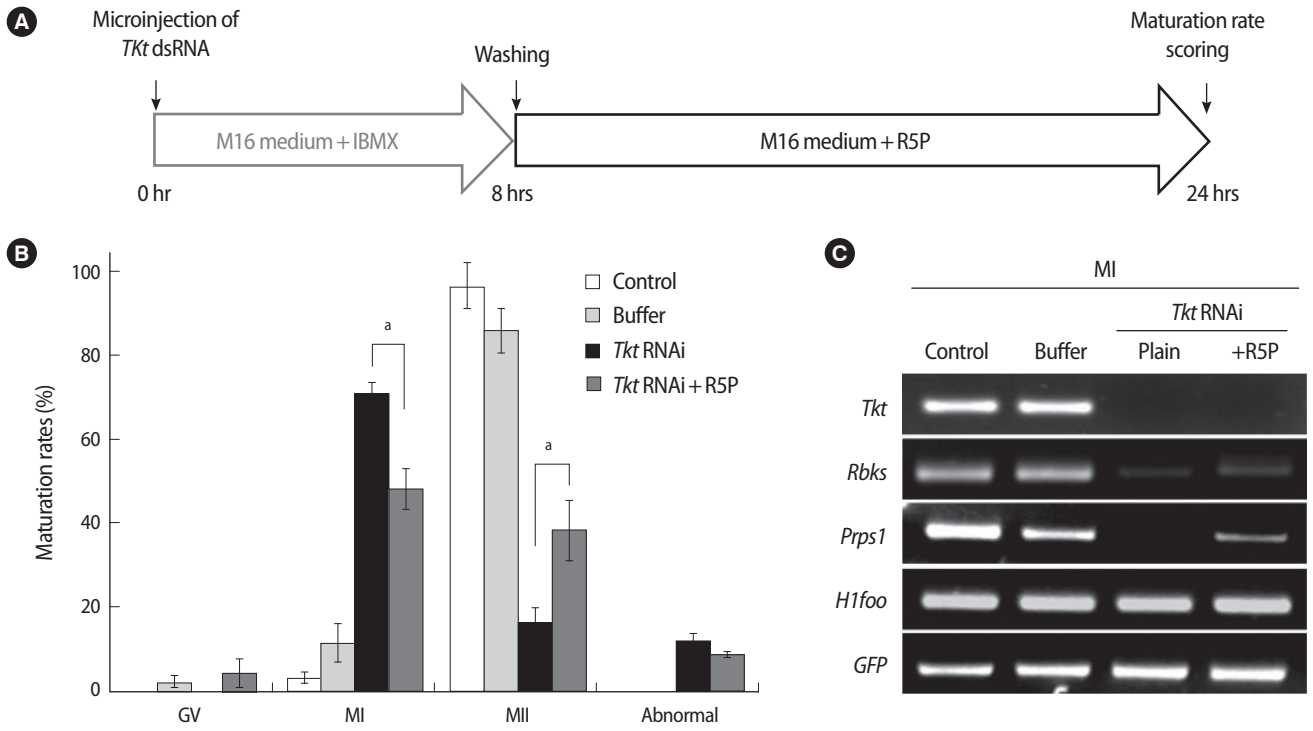

Figure 7. The effect of R5P treatment on the action of *Tkt* RNAi. (A) Schematic diagram of the experimental strategy. After microinjection of *Tkt* dsRNA, the oocytes were cultured in M16 medium supplemented with 3-Isobutyl-1-methylxanthine for 8 hours for complete knock down of *Tkt* followed by a 16 hours culture period in M16 medium containing R5P. (B) Maturation rate in the presence and absence of R5P ($^{a}p < 0.05$ vs. *Tkt* RNAi). The experiments were repeated at least three times (C) RT-PCR analysis showing changes in the expression of enzymes involved in the pentose phosphate pathway by R5P treatment. R5P, ribose-5-phosphate; *Tkt*, transketolase; *Rbks*, ribokinase; *Prps1*, phosphoribosyl pyrophosphate synthetase 1; RT-PCR, reverse transcriptase-polymerase chain reaction; GV, germinal vesicle; MI, metaphase I; MII, metaphase II.

malities in both spindles and chromosomes. Microtubules and microfilaments are required for the dynamic changes that occur during the final stage of meiosis, such as chromosome segregation, spindle anchorage and rotation, and polar body extrusion [17,18]. Therefore, the aberrations in spindles and chromosomes in the oocytes with *Tkt* knocked down offer compelling evidence suggesting that the Tkt and pentose phosphate pathway are necessary for crucial steps in the MI-MII transition, and are closely related to MPF and MAPK activities. At this moment, it has not been determined whether the arrest of the MI-MII transition is a direct result of *Tkt* RNAi or an indirect effect of the affected MPF and MAPK activities after *Tkt* RNAi, or a combination of both.

Resumption of meiotic maturation in oocytes involves changes in many protein kinase and phosphatase activities [19-21]. Among the kinases, MPF and MAPK are well-known major regulators of oocyte meiotic maturation [22-24]. MPF is activated at GVBD and activates chromatin condensation, nuclear membrane breakdown, and the formation of the meiotic spindle [18]. MPF activity controls the formation and position of the spindle in the oocyte [25]. MPF remains active until MI, and the activity declines during the transition between MI and MII, and is maintained at a plateau as the oocytes progress to MII [26]. MAPK is also involved in the regulation of microtubule organization [18,25]. In this study, *Tkt* RNAi treatment resulted in abnormalities in the spindles and chromosomes, with a concurrent decrease in MPF and MAPK activities in the oocytes arrested at MI.

In a previous study, we showed that microinjection of malate dehydrogenase (*Mor2*) dsRNA into oocytes cultured in M16 medium resulted in the arrest of oocyte maturation at the GV (46.6%) and MI (19.4%) stages [27]. Mor2 is an enzyme involved in the tricarboxylic acid (TCA) cycle. In the following study, *Mor2* RNAi oocytes matured to MII (61.9%) when cultured in M199 medium plus other factors, including hormones and growth factors. Thus, the inhibition of the TCA cycle can be overcome by treatment with hormones and growth factors [28]. When we used the same medium containing hormones and growth factors to culture oocytes after *Tkt* RNAi treatment, however, the oocytes did not mature to MII as in the case of *Mor2* RNAi (data not shown). Therefore, it is evident that the abnormalities in the pentose phosphate pathway, unlike those of glycolysis, are not influenced or surmounted by growth factors or hormones in oocytes.

Since the pentose phosphate pathway generates the R5P that is used for the synthesis of nucleic acids, R5P treatment is associated with increased levels of PRPP, and its entry into purine metabolism

has an effect on oocyte maturation [9]. Incubation of oocytes after *Tkt* RNAi in the medium supplemented with R5P resulted in about 20% increase in the MII oocytes, and an increase in the expression of *Rbks* and *Prps1* mRNA. Based on these results, we propose that pentose phosphate pathway substrate supplementation is a suitable method for improving the oocyte maturation rate during *in vitro* culture to mend potential abnormalities of the enzymes.

In conclusion, we have demonstrated that the function of *Tkt* and its related pentose phosphate pathway in the denuded oocytes is critical for the MI-MII transition in completion of, but not for resumption of, meiotic maturation. In addition, the regulation of the pentose phosphate pathway and glycolysis is different from each other. This work elucidated the role that Tkt plays in the regulation of oocyte maturation.

Conflict of interest

No potential conflict of interest relevant to this article was reported.

References

1. Pincus G, Enzmann EV. The comparative behavior of mammalian dggs in vivo and in vitro: I. the activation of ovarian eggs. J Exp Med 1935;62:665-75.
2. Schmitt A, Nebreda AR. Signalling pathways in oocyte meiotic maturation. J Cell Sci 2002;115:2457-9.
3. Comizzoli P, Urner F, Sakkas D, Renard JP. Up-regulation of glucose metabolism during male pronucleus formation determines the early onset of the s phase in bovine zygotes. Biol Reprod 2003;68:1934-40.
4. Downs SM, Humpherson PG, Leese HJ. Meiotic induction in cumulus cell-enclosed mouse oocytes: involvement of the pentose phosphate pathway. Biol Reprod 1998;58:1084-94.
5. Urner F, Sakkas D. Involvement of the pentose phosphate pathway and redox regulation in fertilization in the mouse. Mol Reprod Dev 2005;70:494-503.
6. Salamon C, Chervenak M, Piatigorsky J, Sax CM. The mouse transketolase (TKT) gene: cloning, characterization, and functional promoter analysis. Genomics 1998;48:209-20.
7. Colton SA, Humpherson PG, Leese HJ, Downs SM. Physiological changes in oocyte-cumulus cell complexes from diabetic mice that potentially influence meiotic regulation. Biol Reprod 2003;69:761-70.
8. Cho WK, Stern S, Biggers JD. Inhibitory effect of dibutyryl cAMP on mouse oocyte maturation in vitro. J Exp Zool 1974;187:383-6.
9. Downs SM. Involvement of purine nucleotide synthetic pathways in gonadotropin-induced meiotic maturation in mouse cumulus cell-enclosed oocytes. Mol Reprod Dev 1997;46:155-67.
10. Kim KH, Kim EY, Lee KA. SEBOX is essential for early embryogenesis at the two-cell stage in the mouse. Biol Reprod 2008;79:1192-201.
11. Cascante M, Centelles JJ, Veech RL, Lee WN, Boros LG. Role of thiamin (vitamin B-1) and transketolase in tumor cell proliferation. Nutr Cancer 2000;36:150-4.
12. Hammes HP, Du X, Edelstein D, Taguchi T, Matsumura T, Ju Q, et al. Benfotiamine blocks three major pathways of hyperglycemic damage and prevents experimental diabetic retinopathy. Nat Med 2003;9:294-9.
13. Paoletti F, Mocali A, Tombaccini D. Cysteine proteinases are responsible for characteristic transketolase alterations in Alzheimer fibroblasts. J Cell Physiol 1997;172:63-8.
14. Sax CM, Salamon C, Kays WT, Guo J, Yu FX, Cuthbertson RA, et al. Transketolase is a major protein in the mouse cornea. J Biol Chem 1996;271:33568-74.
15. Xu ZP, Wawrousek EF, Piatigorsky J. Transketolase haploinsufficiency reduces adipose tissue and female fertility in mice. Mol Cell Biol 2002;22:6142-7.
16. Herrick JR, Brad AM, Krisher RL. Chemical manipulation of glucose metabolism in porcine oocytes: effects on nuclear and cytoplasmic maturation in vitro. Reproduction 2006;131:289-98.
17. Maro B, Johnson MH, Pickering SJ, Flach G. Changes in actin distribution during fertilization of the mouse egg. J Embryol Exp Morphol 1984;81:211-37.
18. Verlhac MH, Kubiak JZ, Clarke HJ, Maro B. Microtubule and chromatin behavior follow MAP kinase activity but not MPF activity during meiosis in mouse oocytes. Development 1994;120:1017-25.
19. Han SJ, Chen R, Paronetto MP, Conti M. Wee1B is an oocyte-specific kinase involved in the control of meiotic arrest in the mouse. Curr Biol 2005;15:1670-6.
20. Lincoln AJ, Wickramasinghe D, Stein P, Schultz RM, Palko ME, De Miguel MP, et al. Cdc25b phosphatase is required for resumption of meiosis during oocyte maturation. Nat Genet 2002;30:446-9.
21. Schultz RM, Montgomery RR, Belanoff JR. Regulation of mouse oocyte meiotic maturation: implication of a decrease in oocyte cAMP and protein dephosphorylation in commitment to resume meiosis. Dev Biol 1983;97:264-73.
22. Kanatsu-Shinohara M, Schultz RM, Kopf GS. Acquisition of meiotic competence in mouse oocytes: absolute amounts of p34(cdc2), cyclin B1, cdc25C, and wee1 in meiotically incompetent and competent oocytes. Biol Reprod 2000;63:1610-6.
23. Mitra J, Schultz RM. Regulation of the acquisition of meiotic competence in the mouse: changes in the subcellular localization of cdc2, cyclin B1, cdc25C and wee1, and in the concentration of

http://dx.doi.org/10.5653/cerm.2012.39.2.58

these proteins and their transcripts. J Cell Sci 1996;109:2407-15.
24. Verlhac MH, de Pennart H, Maro B, Cobb MH, Clarke HJ. MAP kinase becomes stably activated at metaphase and is associated with microtubule-organizing centers during meiotic maturation of mouse oocytes. Dev Biol 1993;158:330-40.
25. Brunet S, Maro B. Cytoskeleton and cell cycle control during meiotic maturation of the mouse oocyte: integrating time and space. Reproduction 2005;130:801-11.
26. Abrieu A, Dorée M, Fisher D. The interplay between cyclin-B-Cdc2 kinase (MPF) and MAP kinase during maturation of oocytes. J Cell Sci 2001;114:257-67.
27. Yoon SJ, Koo DB, Park JS, Choi KH, Han YM, Lee KA. Role of cytosolic malate dehydrogenase in oocyte maturation and embryo development. Fertil Steril 2006;86:1129-36.
28. Kim EY, Kim KH, Kim YS, Lee HS, Kim Y, Lee KA. Comparative functional analysis of the malate dehydrogenase (Mor2) during in vitro maturation of the mouse and porcine oocytes. Dev Reprod 2007;11:263-72.